

Electronic structure, photovoltage, and photocatalytic hydrogen evolution with p-CuBi₂O₄ nanocrystals

Geetu Sharma,^a Zeqiong Zhao,^a Pranab Sarker,^b Benjamin A. Nail,^a Jiarui Wang,^a Muhammad N. Huda,^b and Frank E. Osterloh*^a

^a Department of Chemistry, University of California, Davis. One Shields Avenue, Davis, CA, 95616, USA. Phone: (+1)530 754 6242; Fax: (+1)530 752 8995; E-mail: fosterloh@ucdavis.edu.

^b University of Texas Arlington, Department of Physics, Arlington, TX 76019, USA.

Supporting Information (4 pages)

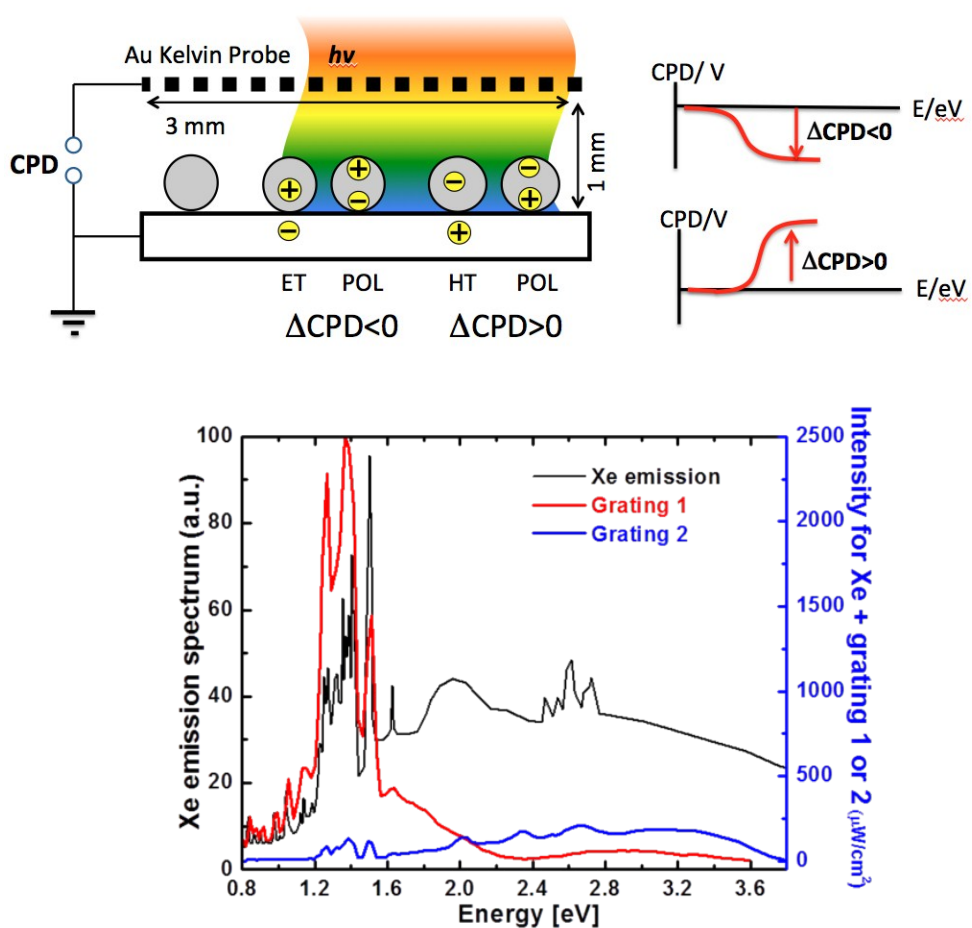


Figure S1. SPS measurement configuration and emission spectrum of light source (Grating 2 was used for all measurements)

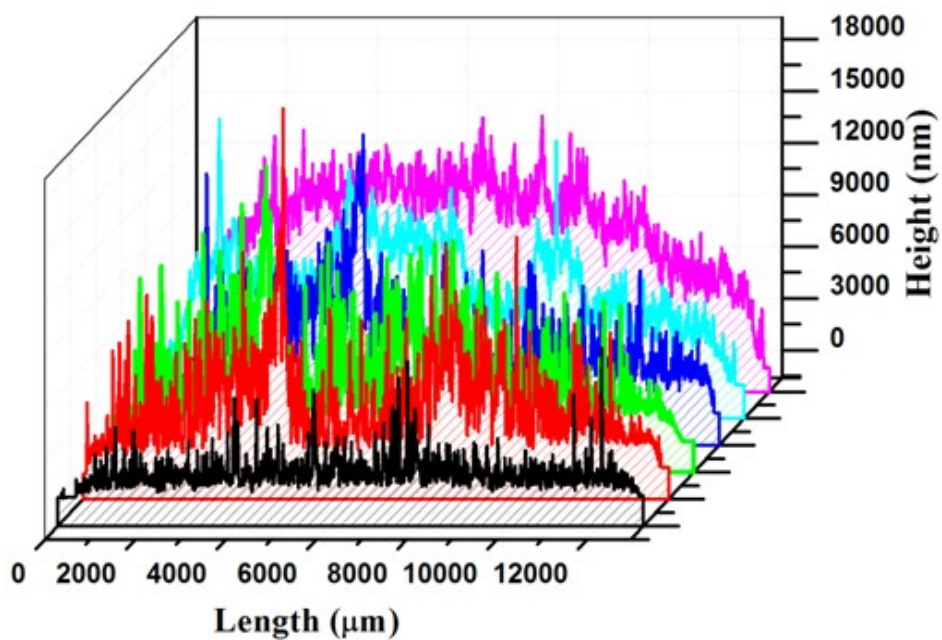


Figure S2. Profilometry scans of CuBi₂O₄ films on FTO with different thickness.

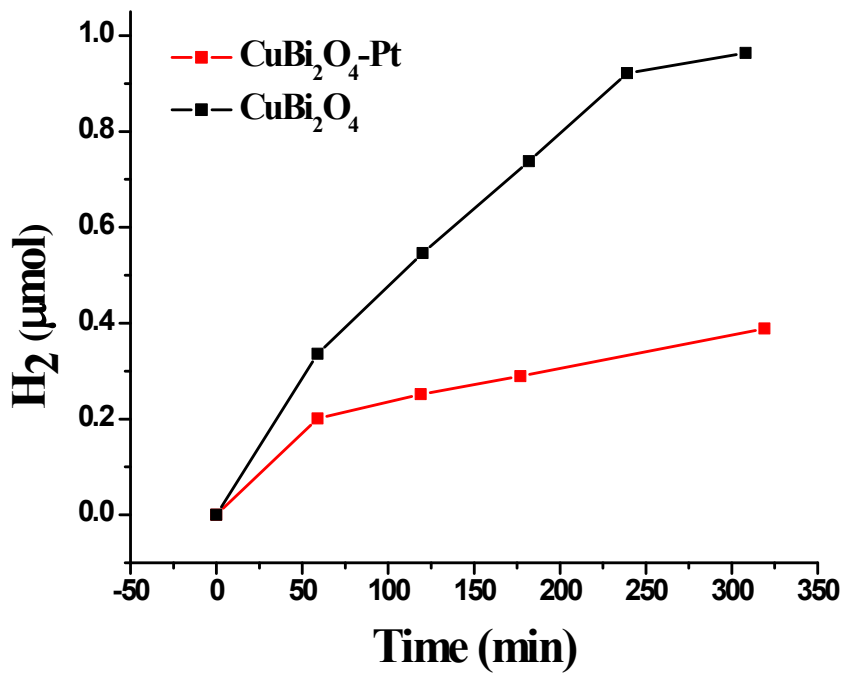


Figure S3. H₂ evolution from 50 mg CuBi₂O₄ nanoparticles in 100 mL of aqueous methanol (20% v/v) solution under visible light (> 400 nm, 240 mW cm⁻² at flask), before and after addition of a Pt cocatalyst. The lower activity of the platinated material is attributed to photocorrosion of CuBi₂O₄ during photodeposition of Pt. Conditions: 50 mg of CuBi₂O₄ was dispersed in a solution of H₂PtCl₆ (1 mol % Pt) and 10% methanol in water and irradiated two hours with unfiltered light from a 300 W Xe arc lamp. Platinated powders were washed repeatedly with pure water before use.

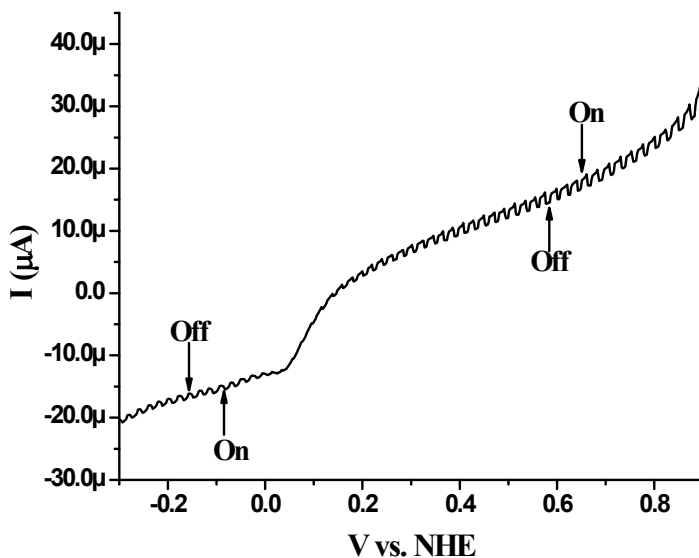


Figure S4. Photoelectrochemical scan on CuBi₂O₄ nanocrystal film on FTO substrate in 0.1 M K₂SO₄ under Xe – illumination (full spectrum, 40 mW cm⁻²).

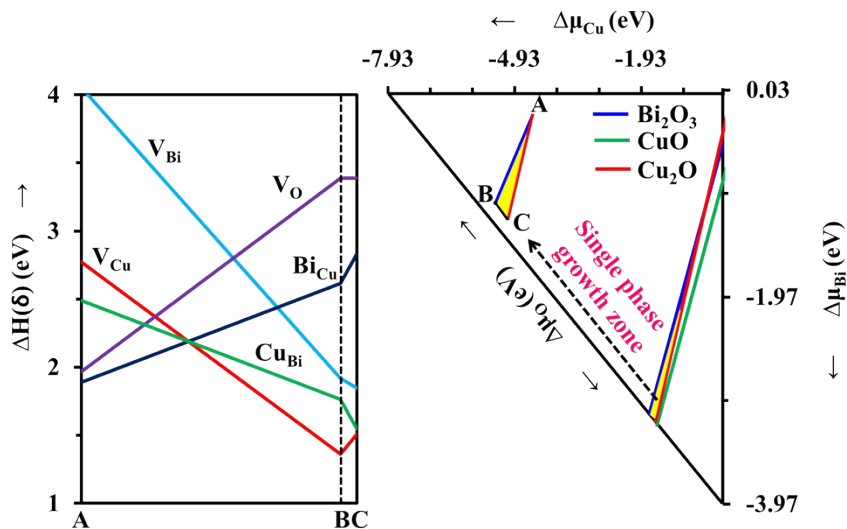


Figure S5: The left figure represents the probability of forming different intrinsic defects in CuBi₂O₄ with respect to its single-phase growth region (see yellow bounded region at right figure); the yellow region in the left figure was achieved using the chemical potential landscape analysis (for detail

methodology, see ref. 1¹). ΔH is the defect formation energy. In the right figure, $\Delta\mu_\alpha$ ($\alpha = \text{Cu}, \text{Bi}, \text{and O}$) axes correspond to growth conditions, from rich ($\Delta\mu_\alpha = 0 \text{ eV}$) to poor ($\Delta\mu_\alpha = \text{formation enthalpy}$), of respective species. The values of A, B, and C in the figure are ($\Delta\mu_{\text{Cu}} = -0.33 \text{ eV}, \Delta\mu_{\text{Bi}} = -0.96 \text{ eV}, \Delta\mu_{\text{O}} = -1.42 \text{ eV}$), ($\Delta\mu_{\text{Cu}} = -1.74 \text{ eV}, \Delta\mu_{\text{Bi}} = -3.10 \text{ eV}, \Delta\mu_{\text{O}} = 0 \text{ eV}$), and ($\Delta\mu_{\text{Cu}} = -1.60 \text{ eV}, \Delta\mu_{\text{Bi}} = -3.17 \text{ eV}, \Delta\mu_{\text{O}} = 0 \text{ eV}$), respectively.

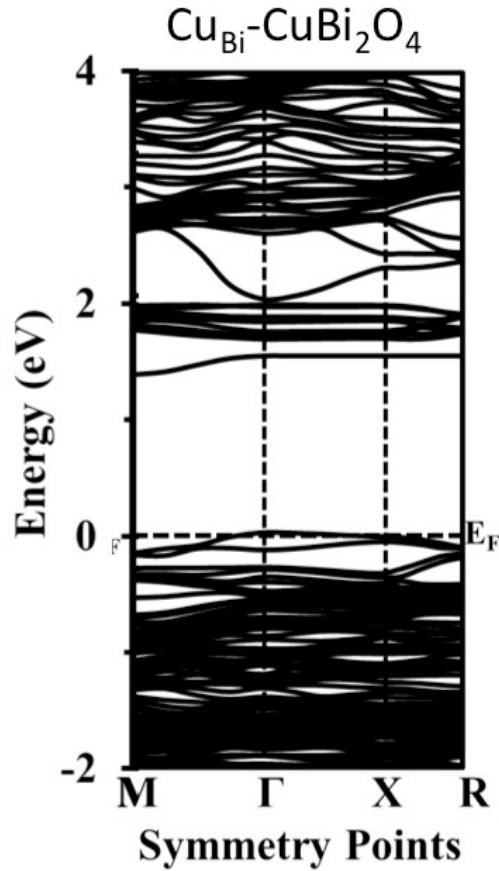


Figure S6. The DFT+U electronic band structure of $\text{Cu}_{\text{Bi}} - \text{CuBi}_2\text{O}_4$.

Reference:

- 1 P. Sarker, M. M. Al-Jassim and M. N. Huda, *J. Appl. Phys.*, 2015, **117**, 035702.